PACS: 81.40.Vw

V.N. Varyukhin, T.T. Moroz, V.S. Abramov

INFLUENCE OF PRELIMINARY HYDROSTATIC PRESSURE TREATMENT ON THE ELECTRICAL RESISTANCE AND STRUCTURE OF AMORPHOUS $Co_{67}Cr_7Fe_4Si_8B_{14}$ ALLOY

Donetsk Institute for Physics and Engineering named after A.A. Galkin, National Academy of Sciences of Ukraine
72 R. Luxemburg st., Donetsk, 83114, Ukraine

Received November 25, 2009

The effect of preliminary pressure treatment (PT) on peculiarities of changes in electrical resistance R and structure of the amorphous $Co_{67}Cr_7Fe_4Si_8B_{14}$ alloy during a constant-rate heating to temperatures under the crystallization onset temperature has been studied using the resistance measurement and X-ray diffraction (XRD) methods. Preliminary PT has been done at 300 K (P = 1 GPa) in the repetitive static mode for different number N of loading cycles (N = 1, 3, 5).The XRD data show that the amorphous state of the studied alloy is conserved but its fine structure has changed after PT, as observed by variation of halo parameters. It has been found that after PT with an increase in the number N of loading cycles, the ordering of the original amorphous structure is enhanced, while after heating from 828 to 843 K, the disordering growth is enhanced. Anomalies of R (a minimum at 497 K and a sharp rise in the range of 800–843 K) observed in the dependence R(T) of the original amorphous alloy are present after the PT too. They seem to be due to structural phase transitions of amorphous alloy during heating.

Keywords: hydrostatic pressure, amorphous alloy, structure, halo, electrical resistance

1. Introduction

Amorphous metal alloys (AA) refer to thermodynamically nonequilibrium systems in which the structure relaxation and crystallization processes develop under an external influence, such as temperature, pressure, deformation, etc. High-pressure effect on AA crystallization process gives changes in the temperature T_s of crystallization onset and in the sequence of crystalline phase precipitation, thus favoring the formation of structures with a more close packing of atoms. Most literary data [1–3] show that there is an increase in T_s with pressure growth during heating the AA under pressure. The conventional explanation is as follows. As the diffusion-controlled process of AA crystallization proceeds by the nucleation and the growth mechanism, the pressure results in decreasing the diffusion mobility of atoms and, as a consequence, in a more difficult crystallization proc-

ess, i.e. in T_s increase. However, for a number of alloys ($Ti_{80}Si_{20}$, $Al_{89}La_6Ni_5$) an opposite effect is observed, viz. T_s decreases with pressure increase. A thermodynamic model [4] has been proposed to describe the nucleation process during AA crystallization under pressure with a special attention paid to the formation (especially at early stages) of the amorphous–crystalline phase interface. Calculations done within the model explain both the increase (for amorphous Se and $Ni_{80}P_{20}$) and decrease (for $Al_{89}La_6Ni_5$) of AA thermal stability under pressure.

Of obvious interest is the behaviour of some AA of the Co–Fe–Cr–Si–B system in the process of crystallization. According to Cziraki et al. [5], the crystallization of Fe–M–B–Si (M = Co, Cr, Mn, Ni) amorphous alloys results in a specific microstructure which is presumably composed of nanocrystals 1–3 nm in diameter. In addition, the process is accompanied by a pronounced heat release and anomalous rise in the resistance R in the corresponding temperature range. The amorphous $Co_{67}Cr_7Fe_4Si_8B_{14}$ alloy under study shows a similar behaviour of R during heating. We have studied the effect of preliminary pressure treatment (PT) on nanocrystallization process for this alloy [6]. It has been shown that after PT, the thermal stability of the alloy decreases. Nanocrystallization mechanism, sequence of the crystalline phase precipitation and the phase composition of the crystallization products do not change. And there is a tendency to reducing the crystal dimensions of the stable crystalline phase.

This paper is aimed at studying the influence of hydrostatic pressure treatment on peculiarities of changes in electrical resistance and structure of the amorphous $Co_{67}Cr_7Fe_4Si_8B_{14}$ alloy during a constant-rate heating to temperatures under the crystallization onset temperature.

2. Experimental

The investigated was the amorphous $Co_{67}Cr_7Fe_4Si_8B_{14}$ alloy prepared by melt spinning to have a 12 mm wide and 0.03 mm thick tape. Preliminary PT was done at 300 K in a repetitive static mode with the number N = 1, 3 5 of loading cycles and at P = 1 GPa. The samples having the dimension 0.03 × 1.5 × 25 mm were placed along the axis of high-pressure chamber whose cavity was filled with a working fluid. The chamber was loaded by means of a hand-power press. The rate of pressure pick up – 15 MPa/s, the rate of unloading – 6 MPa/s, the pressure was maintained for 180 s, and nonhydrostaticity along liquid column – $4 \cdot 10^{-3}$ GPa/mm for P = 1 GPa.

The resistance measurement and XRD methods have been used in this work. The electrical resistance R of the samples was measured (the error of $\pm 2 \cdot 10^{-5}$ Ω) by a standard four-probe dc method. The voltage at the sample (proportional to ΔR) and temperature T (accuracy ±1.5 K) during the heating were recorded by a dc six- channel KSP-4 potentiometer. The heating rate was maintained constant at 0.25 K/s. The results were analyzed in the form of $R(T)$ dependence normalized to value R_0 measured at 300 K prior the sample heating. XRD photographs were taken from polished sections in an RKU-114 Debye–Scherrer powder camera (URS-55 X-ray generator, filtered cobalt radiation).

3. Results and discussion

The XRD data represented in Fig. 1 (curve *1*) show the initial state of the alloy studied to be amorphous: microphotogram of the sample shows a broad diffuse halo; there are no peaks corresponding to crystal phases. After preliminary PT the amorphous state is conserved but its fine structure alters as shown by changes in halo parameters such as the integrated width β_1 and the relative integrated intensity ξ ($\xi = I_{halo}/(I_{halo} + I_{incoh})$, where I_{halo} and I_{incoh} are integrated intensities of the halo and the incoherent scattering of X-rays from the studied sample). With an increase in the number N of PT loading cycles, β_1 decrease*s* while the degree of structure ordering ξ increases. The angle corresponding to the maximum of halo does not change and responds to that of coordination sphere of 0.1978 nm the most probable radius close to the position of the most intense line of Co_3B phase.

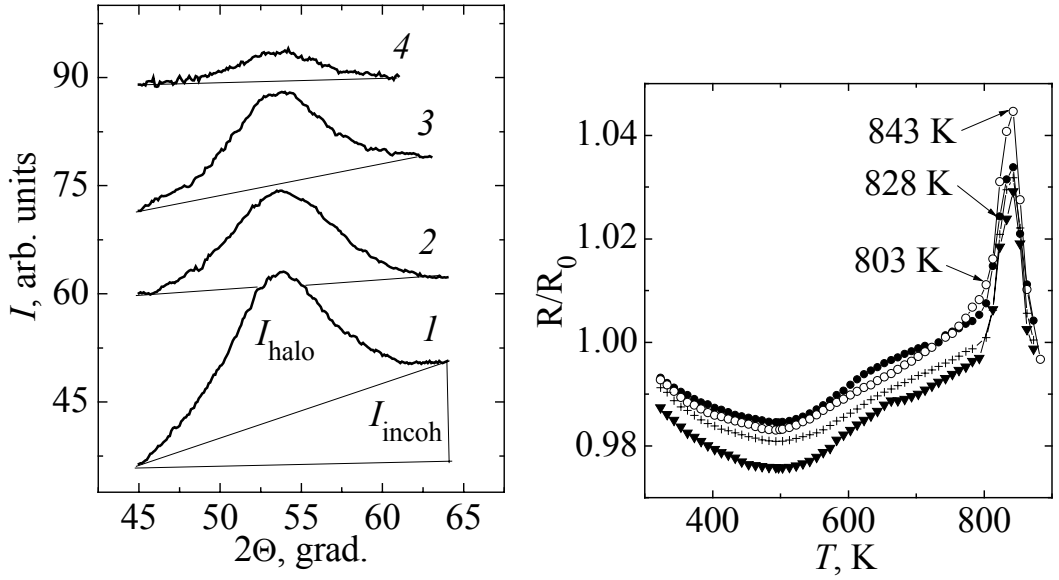

Fig. 1. Microphotograms from $Co_{67}Cr_7Fe_4Si_8B_{14}$ alloy without the PT (curve *1* – $\xi = 0.5$, $\beta_1 = 7.8°$) and after the PT: *2* – $N = 1$, $\xi = 0.8$, $\beta_1 = 7.4°$; *3* – $N = 3$, $\xi = 0.6$, $\beta_1 = 7.2°$; *4* – $N = 5$, $\xi = 0.8$, $\beta_1 = 5.8°$

Fig. 2. Temperature dependences of R/R_0 for $Co_{67}Cr_7Fe_4Si_8B_{14}$ alloy (the heating rate of 0.25 K/s) without (●) and after the PT for $N = 1$ (○), 3 (+), 5 (▼)

Fig. 2 illustrates the curves of changes in relative resistance R/R_0 of alloy samples (without and past PT) for a constant rate heating to 873 K. The curves consist of two distinct parts (300–773, 773–873 K). At first part, the attention is turned to a smooth transition from negative to positive values of the temperature coefficient of resistance with the minimum R/R_0 (for the alloy without PT) at $T_m = 497$ K. For the second range, R/R_0 shows a sharp maximum at $T_s = 843$ K.

The temperature T_m is changed insignificantly for the samples after PT at $N = 1$ and $N = 3$, whereas it transforms into the temperature plateau of 493–503 K for

that after PT at $N = 5$. The value T_s for all the samples (with no and past PT) remains constant and equals 843 K. And the larger the N of PT cycles the lower are corresponding R/R_0 curves for the samples past a preliminary PT.

The method of quenching was used to follow the evolution of diffraction patterns from samples (without and past the PT) in the initial and heated states. The samples were heated at the same (0.25 K/s) rate to temperatures corresponding to the singled out points (Fig. 2, curve *1*), water-quenched, then the XRD analysis was performed. The results are shown in Figs. 3–5. The samples were heated once more to 873 K, the resulting temperature dependences of R/R_0 are illustrated in Fig. 6.

Within the cluster model and the representation on the presence of multiminimum potential, the AA structure could be represented as an ensemble of clusters confined by more or less rigid bonds and of an intercluster layer. Then the diffraction pattern from the AA samples is a result of X-ray scattering superposition from those components of the structure. The intercluster layer is the main contributor to the incoherent X-ray scattering. With the above representations taken into consideration we have constructed curves $I_1(2\theta)$ shown in Fig. 3 and 4 by subtraction from the X-ray scattering intensity $I(2\theta)$, the incoherent scattering intensity $I_{\text{incoh}}(2\theta)$ for the same (2θ) slip angle of a particular diffraction pattern. To follow changes in curve profiles depending on PT and heating temperature, we show the corresponding symmetric curves $I_2(2\theta)$ by dotted lines. Under the figure,

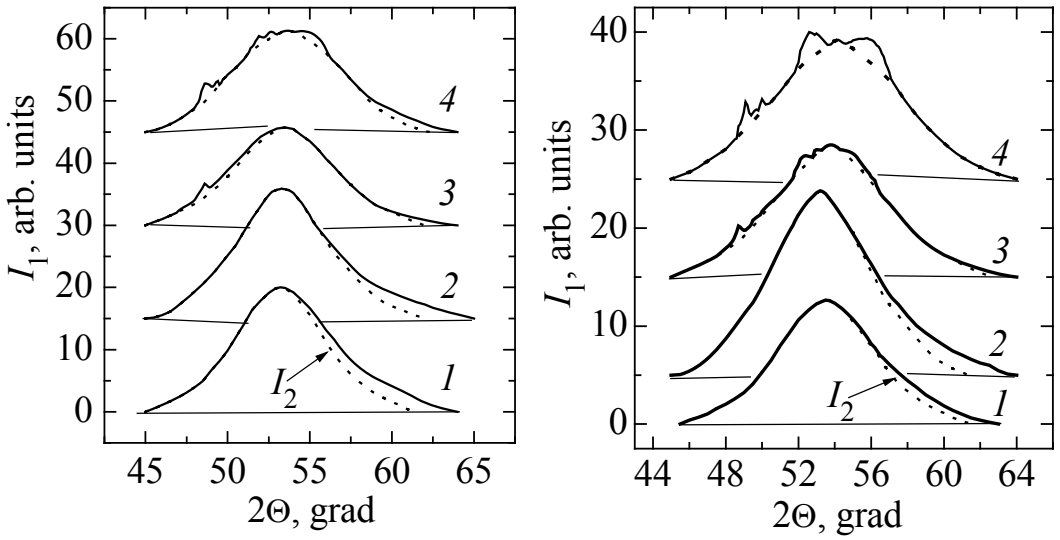

Fig. 3. Microphotograms from $Co_{67}Cr_7Fe_4Si_8B_{14}$ alloy without the PT in as-quenched amorphous state (curve *1* – $2\theta_m$ =53.8°, $\beta_1 = 7.8°$, $\beta_2 = 6.9°$, $\eta = 0.63$) and after heating followed by water quenching: *2* – heating to 803 K, $2\theta_m = 53.5°$, $\beta_1 = 7.7°$, $\beta_2 = 7.1°$, $\eta = 0.63$; *3* – 828 K, $2\theta_m = 53.8°$, $\beta_1 = 8.0°$, $\beta_2 = 7.6°$, $\eta = 0.65$; *4* – 843 K, $2\theta_m = 54.0°$, $\beta_1 = \beta_2 = 8.1°$, $\eta = 0.63$

Fig. 4. Microphotograms from $Co_{67}Cr_7Fe_4Si_8B_{14}$ alloy after the PT ($N = 3$) without (curve *1* – $2\theta_m = 53.8°$, $\beta_1 = 7.2°$, $\beta_2 = 6.8°$, $\eta = 0.56$) and after heating followed by water quenching: *2* – heating to 803 K, $2\theta_m = 53.5°$, $\beta_1 = 7.3°$, $\beta_2 = 6.8°$, $\eta = 0.66$; *3* – 828 K, $2\theta_m = 53.8°$, $\beta_1 = 7.5°$, $\beta_2 = 7.3°$, $\eta = 0.70$; *4* – 843 K, $2\theta_m = 54.0°$, $\beta_1 = \beta_2 = 8.4°$, $\eta = 0.95$

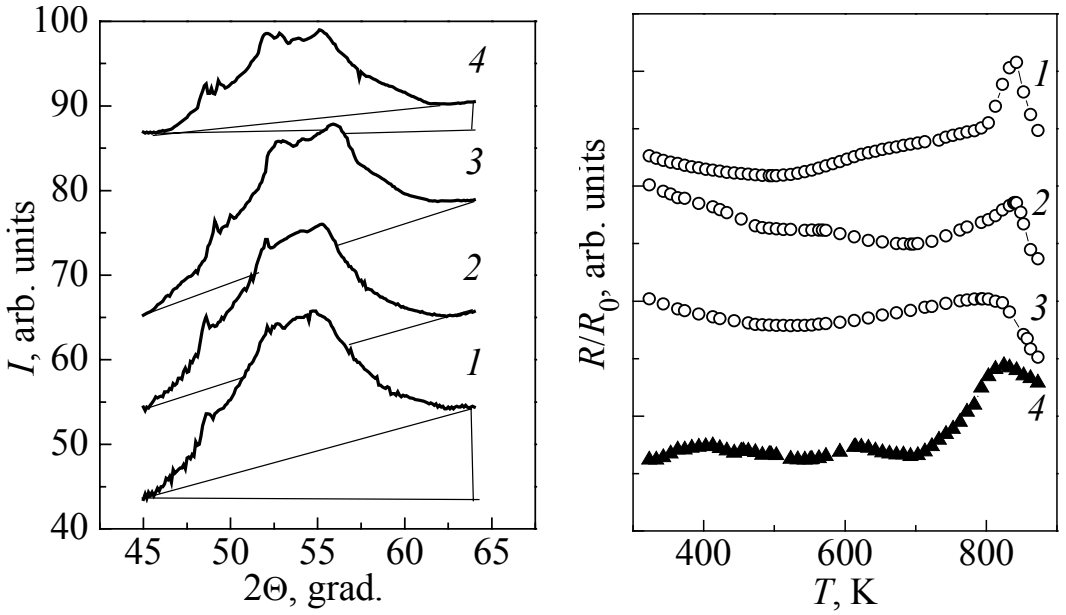

Fig. 5. Microphotograms from $Co_{67}Cr_7Fe_4Si_8B_{14}$ alloy after heating to 843 K followed by water quenching: without the PT (curve *1* – δ = 2.8%) and after the PT for $N = 1$, δ = = 2.8% (curve *2*); $N = 3$, δ = 6.2% (*3*); $N = 5$, δ = 6.7% (*4*)

Fig. 6. Temperature dependences of R/R_0 for $Co_{67}Cr_7Fe_4Si_8B_{14}$ alloy (heating rate 0.25 K/s) without PT in as-quenched amorphous state (curve *1*) and after heating followed by water quenching: *2* – heating to 828 K; *3* – 843 K; *4* – 843 K (after the PT, $N = 5$)

values $2\theta_m$, of the maximum intensity angles, β_1 and β_2 of curves $I_1(2\theta)$ and $I_2(2\theta)$ and values of $\eta = H_{incoh}/H_{coh}$ (H_{incoh}, H_{coh} – the maximum intensities of the incoherent and coherent (halo) X-ray scattering in the studied interval $2\theta = 45–65°$) are shown.

The amorphous state of metal alloys is unstable from thermodynamic point of view, that is why a preliminary PT, the same as any external influence, will, in our opinion, favour the development of structural relaxation process. The XRD results (Figs. 1, 3, 4) show that after PT there are irreversible changes in the as-prepared amorphous alloy structure: an increase in N of the PT cycles, ξ which is a measure of structure ordering, grows, while β_1, β_2 and halo asymmetry decrease. It points to the fact that the processes of ordering and decreasing of the internal stress level are in progress in the original amorphous structure of studied alloy after the PT. We back up the opinion [7] that the irreversible structural relaxation is a process related mainly to a change in the topological short-range order of atoms in AA, it proceeds through the recombination or annihilation of the *n–p* pairs of the structure defects. The *n*-type defects are similar to dispersed free volume elements, and the *p*-type defects are the centers of the positive local density fluctuations of structure and might be considered as the anti-free volume. Under heating the defects are redistributed, most probably they are split on a smaller and more stable ones. Being participants of atomic transfer they may influence the AA thermal stability.

As seen from Figs 3–4, the halo asymmetry decreases and finally it becomes negligible with an increase in the samples (without and after PT) heating temperature to 843 K. Then, magnitude η, a measure of structure disordering, does not change practically for samples without the PT, but it grows with an increase in N of the preliminary PT cycles. At the temperature of 843 K there is, on the one hand, the maximum of R on the R/R_0 curves (Fig. 2) and, on the other hand, on the halo background there are clear indications of the crystal phases (Fig. 5). The volume fraction δ of the crystal phases in the samples after the PT for $N = 3$ and $N = 5$ is twice as large as in that with no the PT and after it for $N = 1$ ($\delta = I_{cr}/(I_{cr} + I_{halo})$; I_{cr}, I_{halo} – integrated intensities of the X-ray scattering from the crystal and amorphous phases). The latter circumstance gives grounds to assume that after the preliminary PT ($N = 3$ and $N = 5$) the thermal stability of the alloy is decreased.

The sharp rise in R (Fig. 2) observed near T_s in some Co-, Ni-, and Zr-based AA [5,8,9] is mainly explained by two reasons. First, by the process of nanocrystallization which occurs, according to authors [5] simultaneously throughout the sample via composition fluctuations on a wavelength of 10–30 Å and leads to a rise in electrical resistance similar to that during the aging of crystalline alloys, which results from the formation of Guinuer–Preston zones. However, the electron-microscope examination revealed no crystalline phase in the samples quenched from T_s, and their electron diffraction patterns showed only amorphous halo. In [9], it was assumed that the second reason is a change in the scattering mechanism of conduction electrons near T_s, where the amorphous alloys seem to be similar to overcooled liquids, rather than solid glasses.

Our results can confirm that the first explanation is true: after the heating followed by quenching from 843 K (Fig. 5) in AA structure a crystalline phase has been observed. On the other hand, value of electrical resistance growth $R_{843}/R_{800} \approx 1.03$ (see Fig. 2) is close to the jump in R for Co solid–liquid transition [11]. Besides, the analysis of R/R_0 curves (Fig. 6) shows that a 3% crystal phase presence has, during the reheating, resulted in disappearance of the sharp rise of R, in the samples (without the PT). However for the samples (after PT, $N = 5$) containing 6% crystal phase, (curve *4*) the effect was observed. The shape of curve *4* is very different from that of the initial curve *4* in Fig. 2. As a whole, the behaviour of the R/R_0 curves of Fig. 6 points to a complex character of the mechanism of charge-carrier scattering with their localization and delocalization at structure non-uniformities.

We relate the minimum of R on the R/R_0 curves at temperature T_m (see Fig. 2) to a structural phase transition of the original amorphous state during alloy heating. Similar temperature dependences of R/R_0 were reported for a number of amorphous alloys and were, as a rule, interpreted as those due to changes of the carrier scattering mechanism at structural fluctuations, which are accompanied by the Kondo effect or the Anderson tunneling. If structural units of the amorphous state are magnetic, the temperature of the phase transition may coincide with that of the magnetic transition [11]. For example, from the magnetic susceptibility data for the amorphous $Co_{66.6}Fe_{4.9}Cr_{6.9}Si_{7.6}B_{15}$ alloy of composition close to the pres-

ently discussed one, Degro et al. [12] obtained the magnetic phase transition temperature T_c = 493 K, which is nearly close to the temperature of structural transition (497 K) in our alloy.

4. Conclusion

The XRD data show that the amorphous state of the studied alloy is conserved but its fine structure has changed after PT. It has been found that after PT with an increase in the number N of PT loading cycles, the ordering of the original amorphous structure is enhanced, while after heating from 828 to 843 K, the disordering growth is observed.

Anomalies of the electrical resistance R (the minimum at 497 K and the sharp rise in the range of 800–843 K) in R/R_0 curves for the as-quenched amorphous alloy are conserved after the preliminary PT and are evidently related to structural phase transitions. The behaviour of R for thermally treated samples points to a complex character of the mechanism of carrier scattering at structure defects.

1. *W.K. Wang, H. Iwasaki, C. Suryanarayna, T. Masumoto, K. Fukamichi, Y. Syono, T. Goto*, in: Proc. 4th. Int. Conf. on Rapidly Quenched Metals, Sendai (1981), p. 663.
2. *Y. Ogama, K. Nunogaki, S. Endo, M. Kiritani, F.F. Fujita*, in: Proc. 4th. Int. Conf. on Rapidly Quenched Metals, Sendai (1981), p. 675
3. *B. Varga, A. Lovas, F. Ye, X.J. Gu, K. Lu*, Mater. Sci. Eng. **A286**, 193 (2000).
4. *F. Ye, K. Lu*, Phys. Rev. **B 60**, 7018 (1999).
5. *A. Cziraki, B. Fogarassy, I. Szabo, B. Albert*, in: Proc. 4 th Int. Conf. on Rapidly Quenched Metals, Sendai (1981), p. 691.
6. *V.N. Varyukhin*, *T.T. Moroz, V.S. Abramov, V.G. Synkov, V.P. Kravchenko*, High-pressure Physics and Engineering **13**, № 2, 7 (2003) (in Russian).
7. *T. Egami, V. Vitek, D. Srolovitz*, in: Proc. 4 th Int. Conf. on Rapidly Quenched Metals, Sendai (1981), p. 517.
8. *K. Fukamihi, H.M. Kimura, T. Masumoto*, J. Appl. Phys. **52**, 2872 (1981)
9. *O. Haruyama, H.M. Kimura, A. Inoue*, Mater. Sci. Eng. **A226–228**, 209 (1997)
10. *K. Handrich and S Kobe,* Amorphe Ferro und Ferrimagnetika, Akademie, Berlin (1980). Translated under the title Amorfnye Ferro- i Ferrimagnetiki, Mir, Moscow (1982), p. 130–132.
11. *A. Ubbelode*, Melting and Crystal Structure, Calderon Press, Oxford (1965). Translated under the title Plavlenie i Kristallicheskaya Struktura, Mir, Moscow (1969), p. 231.
12. *J. Degro, P. Vojtanik, J. Filipensky, P. Duha*j, J. Magn. Magn. Mater. **117**, 251 (1992).

В.М. Варюхін, Т.Т. Мороз, В.С. Абрамов

ВПЛИВ ПОПЕРЕДНЬОЇ ОБРОБКИ ГІДРОСТАТИЧНИМ ТИСКОМ НА ЕЛЕКТРИЧНИЙ ОПІР ТА СТРУКТУРУ АМОРФНОГО СПЛАВУ $Co_{67}Cr_7Fe_4Si_8B_{14}$

Методами резістометрії та рентгеноструктурного аналізу (РСА) вивчено вплив попередньої обробки тиском (ОТ) на особливості зміни електричного опору R та структуру аморфного сплаву при нагріванні з постійною швидкістю до температур, які не перевищують температуру початку кристалізації. ОТ проведено при кімнатній температурі у повторно-статичному режимі з різним числом N циклів навантаження (N = 1, 3, 5) при тиску P = 1 GPa. За даними РСА, після ОТ аморфний стан сплаву, що вивчається, зберігається, але тонка структура гало змінюється. Показано, що зі зростанням N циклів ОТ зростає упорядкування, а при нагріванні в интервалі 828–843 K – розупорядкування вихідної структури сплаву. Аномалиії R (мінімум при 497 K та різке зростання в межах 800–843 K), які спостерігаються на залежності $R(T)$ вихідного аморфного сплаву, після ОТ зберігаються та пов′язані, напевно, зі структурними фазовими перетвореннями аморфного сплаву у процесі нагрівання сплаву.

Ключові слова: гідростатичний тиск, аморфний сплав, структура, гало, електричний опір

В.Н. Варюхин, Т.Т. Мороз, В.С. Абрамов

ВЛИЯНИЕ ПРЕДВАРИТЕЛЬНОЙ ОБРАБОТКИ ГИДРОСТАТИЧЕСКИМ ДАВЛЕНИЕМ НА ЭЛЕКТРИЧЕСКОЕ СОПРОТИВЛЕНИЕ И СТРУКТУРУ АМОРФНОГО СПЛАВА $Co_{67}Cr_7Fe_4Si_8B_{14}$

Методами резистометрии и рентгеноструктурного анализа (РСА) изучено влияние предварительной обработки давлением (ОД) на особенности изменения электрического сопротивления R и структуры аморфного сплава $Co_{67}Cr_7Fe_4Si_8B_{14}$ при нагреве с постоянной скоростью до температур не выше температуры начала кристаллизации. ОД проведено при комнатной температуре в повторно-статическом режиме с разным числом N циклов обработки (N = 1, 3, 5) при давлении P = 1 GPa. По данным РСА, после ОД аморфное состояние изучаемого сплава сохраняется, но тонкая структура гало изменяется. Показано, что с ростом N циклов ОД растет упорядочение, а при нагреве в интервале 828–843 K – разупорядочение исходной аморфной структуры сплава. Аномалии R (минимум при 497 K и резкий рост в окрестности 800–843 K), наблюдаемые на зависимости $R(T)$ исходного аморфного сплава, после ОД сохраняются и связаны, по-видимому, со структурными фазовыми переходами в процессе нагревания сплава.

Ключевые слова: гидростатическое давление, аморфное состояние, структура, гало, электрическое сопротивление